

UNNS Substrate Research Program | Working Manuscript | April 2026

Emergent Dimensionality in the UNNS Substrate: Connectivity Margin as the Generator of Observable Degrees of Freedom

From Structural Regime Theory to the Origin of Dimensionality

UNNS Substrate Research Program

`unns.tech`

Companion manuscripts: Interaction Unification · Phase Mapping of Structural Regimes · Structural Response to Constant Deformations · Percolative Realizability Principle · Dual Observability

Instruments: STRUC-I v1.0.4 · STRUC-PERC-I v2.4.1 · Field Generator v1.0 · `unns_scaling_extractor.py` · `transition_generator.py`

Corpus: 93 datasets · 22,817 evaluations · 11 physical domains · 35 systems (extended 4-domain corpus)

April 2026

Abstract

We propose a structural derivation of dimensionality within the UNNS Substrate framework. Building on the Universal Structural Law (USL), the Dual Observability Theorem, the Percolative Realizability Principle (PRP), and the empirically supported theory of connectivity margin $m(L)$, we show that dimensionality is not a primitive geometric property but an emergent observable determined by the set of structurally admissible degrees of freedom.

We define degrees of freedom as admissible independent structural transformation axes (where independence is defined with respect to non-redundant variation in the structural state $\mathcal{S}(L)$) and demonstrate that their accessibility is governed by the connectivity margin. Effective dimensionality is thus a regime-dependent quantity, with $\dim_{\text{eff}}(L) = |\mathcal{D}(m(L), \bar{\rho}, \mathcal{R})|$. This framework provides a structural reinterpretation of hidden or compactified dimensions as suppressed degrees of freedom, and connects dimensionality directly to interaction regimes, operator response, and structural stability.

We further extend the framework to observable scaling: effective dimensionality constrains the asymptotic scaling behaviour of physical systems. The central claim is that scaling exponents, decay laws, and correlation families are selected not arbitrarily, but from a family determined by $(\dim_{\text{eff}}(L), m(L))$. Dimensionality thus becomes experimentally meaningful: not a geometric primitive, but a predictor of measurable scaling structure. The theory yields falsifiable predictions regarding exponent shifts, symmetry activation, and scaling transitions under structural deformation.

The framework is consistent with the UNNS corpus, including universal structural rigidity under (α, μ) deformation (zero inter-class transitions across 22,817 evaluations) and representation-dependent realizability variation.

Contents

1	Introduction: The Dimensionality Problem	3
1.1	Why Dimension Is Assumed, Not Derived	3
1.2	What the UNNS Substrate Provides	3
1.3	The Question Addressed	3
2	Structural Preliminaries: Minimal Recap	3
3	Degrees of Freedom as Structural Objects	4
3.1	Definition and Motivation	4
3.2	Relation to Realizability Coordinates	4
4	Margin-Dependent Accessibility of Degrees of Freedom	5
4.1	The DOF Activation Functional	5
4.2	Regime Dependence of Accessible DOF	5
5	Emergent Dimensionality	6
5.1	Definition of Effective Dimensionality	6
5.2	Dimensionality Hierarchy Across Regimes	7
6	Diagram: Regime to DOF to Dimension	7

7	Reinterpretation of Extra Dimensions	8
7.1	Mapping Physics Concepts to UNNS	8
8	Connection to Interaction Hierarchy	8
8.1	DOF Activation Profiles of Interactions	8
9	Operator Activation of Degrees of Freedom	9
9.1	Operators as DOF Activators	9
9.2	Operator Regime Behaviour and Structural Attractors	10
9.3	Spectral Invariance and Encoding Collapse	12
10	The Dimensional Selection Principle	17
11	Empirical Alignment with Corpus Results	17
11.1	Multi-Domain Corpus Results and Theorem Correspondence	19
11.2	On the Non-Derived Minimum Margin Function	22
12	From Effective Dimensionality to Observable Scaling	24
12.1	Scaling Selection Principle	24
12.2	Exponent Functions and Observable Response	24
12.3	Worked Example: α -Driven DOF Activation and Scaling	25
12.4	Observable Meaning of DOF Activation	25
13	Renormalization Interpretation of Structural Deformation	26
14	Predictions and Falsifiability	27
15	Relation to Existing Theories	28
15.1	General Relativity	28
15.2	String Theory	29
15.3	Quantum Field Theory	29
16	Conclusion	29
A	Proof of Theorem 5.1 (Detailed)	31
B	DOF Activation Functional: Threshold Form Derivation	31

1 Introduction: The Dimensionality Problem

1.1 Why Dimension Is Assumed, Not Derived

Modern physics treats dimensionality as a fundamental property of space. From the three spatial dimensions of everyday experience to the four-dimensional spacetime of general relativity, dimension is taken as a primitive input. Frameworks such as Kaluza–Klein theory and string theory introduce additional spatial dimensions to achieve unification, typically assuming these dimensions are compactified or otherwise hidden. The question of why the observable universe has the dimensionality it does is not answered — it is parameterised.

1.2 What the UNNS Substrate Provides

The UNNS Substrate offers a fundamentally different starting point. Rather than postulating dimensionality, it derives observable structure from constraints on admissible ordered sequences (ladders) under the Universal Structural Law:

$$\text{inv}(P_\varepsilon; L) \leq \nu(V_\varepsilon(L)) \quad (1)$$

The Dual Observability Theorem establishes two independent structural coordinates: admissibility $\bar{\rho}(L)$ and realizability $\mathcal{R}(L)$. The connectivity margin $m(L)$ (distance to the nearest realizability-class boundary) governs stability, capacity, and interaction classification.

1.3 The Question Addressed

This paper addresses the following question:

What determines the number of effective degrees of freedom observed in physical systems?

We show that dimensionality emerges from structural admissibility and is governed by the connectivity margin. Within the UNNS framework, dimensionality is not primary but derived.

2 Structural Preliminaries: Minimal Recap

We collect only the definitions required for the dimensionality argument. Full derivations are in the companion manuscripts.

Definition 2.1 (Ladder and Gap Sequence). A *ladder* is a finite ordered sequence $L = (x_1 \leq x_2 \leq \dots \leq x_n)$, $n \geq 3$, $x_i \in \mathbb{R}$. Its *gap sequence* is $\Delta = (\Delta_1, \dots, \Delta_{n-1})$, $\Delta_i = x_{i+1} - x_i > 0$.

Definition 2.2 (Structural State). The structural state of an admissible configuration is the pair

$$\mathcal{S}(L) = (\bar{\rho}(L), \mathcal{R}(L)),$$

where $\bar{\rho}(L)$ is the admissibility coordinate (structural pressure) and $\mathcal{R}(L)$ is the realizability coordinate, which includes the realizability class $\mathcal{C}(L) \in \{\text{FULL}, \text{GIANT}, \text{TAIL}, \text{HARD}\}$ and the connectivity threshold κ_{conn} .

Definition 2.3 (Connectivity Margin). Let L have gap sequence Δ and median gap $\tilde{\Delta}$. The *connectivity margin* is

$$m(L) = \min_{\text{decisive } (i,j)} \frac{||\Delta_i - \Delta_j| - \varepsilon(\kappa^*)|}{\tilde{\Delta}},$$

where κ^* is a critical threshold at which the realizability class would change. This measures the distance of the gap vector from the nearest realizability-class boundary.

Principle 1 (Bounded Structural Rigidity of Realizability). *Let $L \in \mathcal{M}_{\text{adm}}$ be an admissible ladder. There exists a finite deformation domain $\Omega_L \subset \mathbb{R}^2$ containing $(\alpha, \mu) = (1, 1)$ such that the realizability class $\mathcal{C}(L)$ and vulnerability graph $G_\kappa(L)$ are invariant over Ω_L . The tested domain $\Omega = [0.80, 1.20]^2$ lies within Ω_L for all 93 corpus datasets (22,817 evaluations), with zero inter-class transitions and zero non-trivial commutators.*

3 Degrees of Freedom as Structural Objects

3.1 Definition and Motivation

The concept of “degree of freedom” in physics is traditionally tied to configuration space dimension, number of independent coordinates, or field components. We replace this with a structural criterion internal to the UNNS framework.

Definition 3.1 (Structural Degree of Freedom). Let $L \in \mathcal{M}_{\text{adm}}$ be an admissible ladder. A *structural degree of freedom* is an admissible independent structural transformation axis in the admissibility manifold \mathcal{M}_{adm} . Formally, a direction δ in the tangent space of \mathcal{M}_{adm} such that variation along δ preserves admissibility while changing the structural state $\mathcal{S}(L)$ in a measurable way. Independence is defined with respect to non-redundant variation in $\mathcal{S}(L)$: two directions δ_1, δ_2 are independent if their associated variations span distinct dimensions of the structural state space.

Remark 1. This definition removes dependence on spatial interpretation. Degrees of freedom are not coordinates in a geometric space — they are modes of structural variation that the system can access while remaining admissible. The key insight is that admissibility constraints *select* which transformation axes are physically realisable. This notion of dimensionality differs from manifold dimension and should be understood as operational rather than geometric.

3.2 Relation to Realizability Coordinates

The realizability coordinate $\mathcal{R}(L)$ provides a natural classification of degrees of freedom. Different realizability classes correspond to different profiles of accessible transformations:

- **FULL** class (deep interior): all structural transformation axes are accessible — maximal degrees of freedom.

- GIANT class: most axes accessible; a small number of directions are suppressed (outlier gaps).
- TAIL class: a dominant backbone of axes remains, but specific directions (corresponding to outlier gaps) are isolated.
- HARD class: severe fragmentation; many axes are inaccessible.

4 Margin-Dependent Accessibility of Degrees of Freedom

4.1 The DOF Activation Functional

We introduce a functional that maps the connectivity margin to the set of active degrees of freedom. Critically, DOF activation depends on *both* structural coordinates: admissibility $\bar{\rho}(L)$ and realizability $\mathcal{R}(L)$.

The functional \mathcal{D} acts as a **threshold selection operator** over admissible structural directions. Each direction δ has an associated activation threshold $m_{\min}(\delta, \bar{\rho}, \mathcal{R})$, and is included in \mathcal{D} if and only if:

$$m(L) \geq m_{\min}(\delta, \bar{\rho}, \mathcal{R}). \quad (2)$$

This formulation is simpler, clearer, and computationally interpretable than a gradient-based inequality. The threshold $m_{\min}(\delta, \bar{\rho}, \mathcal{R})$ may be derived from directional gap variance and local curvature of the realizability boundary (future work).

Definition 4.1 (DOF Activation Functional — Threshold Form). Let L be an admissible ladder with connectivity margin $m(L)$, admissibility coordinate $\bar{\rho}(L)$, and realizability coordinate $\mathcal{R}(L)$. Define the *DOF activation functional* as:

$$\mathcal{D}(m(L), \bar{\rho}, \mathcal{R}) = \{\delta \in T\mathcal{M}_{\text{adm}} \mid m(L) \geq m_{\min}(\delta, \bar{\rho}, \mathcal{R})\},$$

where $m_{\min}(\delta, \bar{\rho}, \mathcal{R})$ is the minimum margin required for direction δ to become accessible given the current admissibility and realizability state. The set $\mathcal{D}(m(L), \bar{\rho}, \mathcal{R})$ is the set of structural transformation axes accessible at margin $m(L)$.

Remark 2 (Interpretation). The functional captures a simple structural fact: as $m(L)$ increases (deeper interior), more transformation axes satisfy the threshold condition because the system is farther from class boundaries. As $m(L) \rightarrow 0$ (approach to boundary), the number of accessible axes shrinks. At $m(L) = 0$ (the boundary itself), only axes with $m_{\min} = 0$ remain accessible. We treat \mathcal{D} as an effectively finite active subset of a high-dimensional admissibility manifold; the ambient dimension of $T\mathcal{M}_{\text{adm}}$ is not specified, but the accessible subset is finite in practice.

4.2 Regime Dependence of Accessible DOF

The accessibility of degrees of freedom follows a clear pattern across margin regimes:

Margin regime	Accessible DOF	Structural interpretation
$m(L) \gg 0$ (deep interior)	Maximal	All transformation axes accessible
$m(L) > 0$ (stable)	High	Most axes accessible
$m(L) \rightarrow 0$ (near boundary)	Reduced	Only axes along the boundary
$m(L) = 0$ (boundary)	Minimal	Only tangent directions

Theorem 4.1 (Monotonicity of DOF Activation). *Let $L \in \mathcal{M}_{\text{adm}}$ be an admissible ladder. For two structural states with margins $m_1 < m_2$ and the same realizability class $\mathcal{C}(L)$, we have:*

$$\mathcal{D}(m_1, \bar{\rho}, \mathcal{R}) \subseteq \mathcal{D}(m_2, \bar{\rho}, \mathcal{R}).$$

That is, the set of accessible degrees of freedom is monotonic non-decreasing in the connectivity margin, provided the realizability class remains unchanged.

Proof sketch. By Definition 4.1, a direction δ is accessible iff $m(L) \geq m_{\min}(\delta, \bar{\rho}, \mathcal{R})$. If $m_2 > m_1$, then any δ with $m_{\min} \leq m_1$ also satisfies $m_{\min} \leq m_2$. Hence $\mathcal{D}(m_1) \subseteq \mathcal{D}(m_2)$. \square \square

Remark 3. Monotonicity is consistent with corpus observations: deeper interior (larger $m(L)$) systems exhibit richer structural behaviour than near-boundary systems. This assumption is used throughout the framework and is now made explicit.

5 Emergent Dimensionality

5.1 Definition of Effective Dimensionality

Definition 5.1 (Effective Dimensionality). Let L be an admissible ladder with active degree-of-freedom set $\mathcal{D}(m(L), \bar{\rho}, \mathcal{R})$ (Definition 4.1). The *effective dimensionality* of the system is the cardinality of this set:

$$\dim_{\text{eff}}(L) = |\mathcal{D}(m(L), \bar{\rho}, \mathcal{R})|.$$

We treat this cardinality as finite in practice because the set of structurally distinct transformation axes is finite for any given ladder; the underlying manifold \mathcal{M}_{adm} may be high-dimensional, but only a finite subset of axes are simultaneously accessible under the margin constraint.

Theorem 5.1 (Dimensionality as an Emergent Observable). *Effective dimensionality $\dim_{\text{eff}}(L)$ is:*

- (i) **Emergent:** *It is not a primitive property but arises from structural admissibility constraints.*
- (ii) **Regime-dependent:** *It varies with the connectivity margin $m(L)$ and realizability class $\mathcal{C}(L)$.*
- (iii) **Structurally determined:** *It is computable from the ladder's gap sequence via the DOF activation functional.*

Proof sketch. Part (i) follows from Definition 3.1, which defines degrees of freedom in terms of admissible transformations — a derived property of \mathcal{M}_{adm} , not a primitive. Part (ii) follows from the margin dependence of $\mathcal{D}(m(L), \bar{\rho}, \mathcal{R})$: as $m(L)$ varies, the set of accessible axes changes. Part (iii) follows from the fact that $m(L)$ is computed directly from the gap sequence (Definition 2.3) and \mathcal{D} is defined in terms of $m(L)$, $\bar{\rho}$, \mathcal{R} , and the threshold m_{min} . \square \square

5.2 Dimensionality Hierarchy Across Regimes

From the corpus-established realizability classes and margin ordering, we obtain a hierarchy of effective dimensionality:

Regime	Margin	dim_{eff}
Strong-like (deep Full)	$m(L) \gg 0$	maximal
EM-like (Full/Giant)	$m(L) > 0$	high
Weak-like (Tail)	$m(L) \rightarrow 0$	reduced
Gravity-like (global)	small positive	minimal/global
HARD (fragmented)	$m(L) = 0$	collapsed

For the gravity-like regime, "global modes" refer to transformation axes that affect the ladder uniformly rather than locally — for example, a uniform scaling of all gap values or a global translation of the entire spectrum. These axes remain accessible even when local structural variations are suppressed near the boundary.

6 Diagram: Regime to DOF to Dimensionality

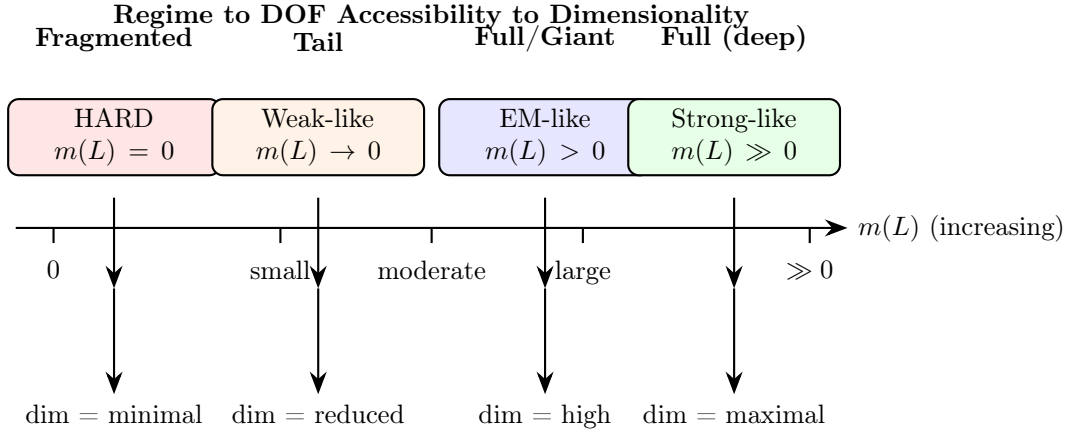


Figure 1: Regime classification as a function of connectivity margin $m(L)$, mapping to accessible degree-of-freedom sets and effective dimensionality. As $m(L)$ increases from 0 (HARD) to $\gg 0$ (deep Full), the system transitions through weak-like (Tail) and EM-like (Full/Giant) regimes, with dimensionality increasing from collapsed/minimal to maximal.

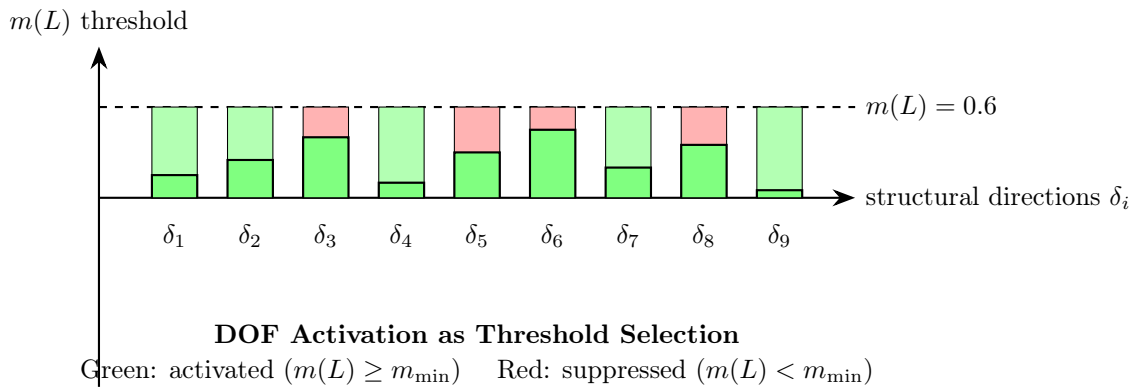


Figure 2: DOF activation as a threshold selection process over structural transformation axes δ_i . Each axis has an associated minimum margin $m_{\min}(\delta_i)$. Axes with $m_{\min} \leq m(L)$ are activated (green); axes with $m_{\min} > m(L)$ are suppressed (red). Effective dimensionality $\text{dim}_{\text{eff}}(L)$ is the number of activated axes.

7 Reinterpretation of Extra Dimensions

7.1 Mapping Physics Concepts to UNNS

The framework provides a structural reinterpretation of concepts from higher-dimensional physics:

Standard concept	UNNS reinterpretation
Compactified dimensions	Suppressed degrees of freedom (low margin)
Higher-dimensional space	High-margin regime
Dimensional reduction	Approach to boundary ($m(L) \rightarrow 0$)
Hidden dimensions	Latent DOF not yet activated
Large extra dimensions	Margin regime with broad DOF accessibility

Theorem 7.1 (Structural Reinterpretation of Compactification). *What is called “compactification” in string theory or Kaluza–Klein theory corresponds, in the UNNS framework, to degrees of freedom that are structurally suppressed because the system lies near a realizability boundary ($m(L) \approx 0$) along those specific transformation axes. These DOF are not geometrically small — they are structurally inaccessible.*

Proof sketch. Compactification in standard physics posits that extra dimensions are curled up at the Planck scale, making them undetectable at low energies. In the UNNS framework, a suppressed degree of freedom is one for which $m_{\min}(\delta) > m(L)$. As $m(L)$ increases (deeper interior), more axes become accessible. The “scale” of compactification is reinterpreted as the margin distance to the boundary along that axis. \square \square

8 Connection to Interaction Hierarchy

8.1 DOF Activation Profiles of Interactions

From the Interaction Unification manuscript, the four fundamental interactions are classified as asymptotic regimes of the margin-parameterised functional $\Phi(m(L), r, \chi(L))$. We

now extend this: each interaction regime corresponds to a distinct DOF activation profile.

Theorem 8.1 (Interaction to DOF Profile). *Let $m(L)$ be the connectivity margin of a system. The interaction regime (strong, EM, weak, gravity) determines and is determined by the active DOF set $\mathcal{D}(m(L), \bar{\rho}, \mathcal{R})$. Specifically:*

- (i) **Strong** ($m(L) \gg 0$): *maximal DOF activation — all structural transformation axes accessible.*
- (ii) **EM** ($m(L) > 0$): *scale-invariant DOF set — most axes accessible, weak scale dependence.*
- (iii) **Weak** ($m(L) \rightarrow 0$, local): *boundary-local DOF restriction — only axes tangent to the boundary remain accessible.*
- (iv) **Gravity** ($m(L) \rightarrow 0^+$, global): *corresponds to the minimal/global DOF regime in the UNNS interpretation — the accessible set consists of the global geometric modes (axes that affect the ladder uniformly).*

Proof sketch. From the asymptotic classification in the Interaction Unification manuscript, each interaction regime corresponds to a distinct functional form of Φ . The DOF activation functional $\mathcal{D}(m(L), \bar{\rho}, \mathcal{R})$ inherits this classification because the number of accessible axes is monotonic in $m(L)$ (Theorem 4.1). The deep interior ($m(L) \gg 0$) maximises accessibility; the boundary ($m(L) \rightarrow 0$) minimises it. The four regimes map to distinct intervals of $m(L)$, hence to distinct DOF profiles. Gravity occupies the small-positive-margin regime, which is distinct from the $m(L) = 0$ HARD boundary. \square \square

9 Operator Activation of Degrees of Freedom

9.1 Operators as DOF Activators

The Structural Response to Constant Deformations manuscript establishes that the α operator (scale/shape) is structurally active while the μ operator (translation/intensity) is realizability-inert. We now interpret this as differential DOF activation.

Definition 9.1 (Operator DOF Activation). Let \hat{O}_c be a structural deformation operator (e.g., \hat{O}_α or \hat{O}_μ). The *DOF activation induced by \hat{O}_c* is the map

$$\Delta_c : \mathcal{D}(m(L), \bar{\rho}, \mathcal{R}) \mapsto \mathcal{D}(m(L)', \bar{\rho}', \mathcal{R}')$$

where $m(L)' = m(L)(\hat{O}_c(L))$ is the margin after deformation.

Theorem 9.1 (Operator-Specific DOF Activation). *Based on the corpus-established operator separation:*

- (i) *The α operator can activate new degrees of freedom in near-boundary systems: for systems with $m(L) \approx 0$, increasing α moves the system deeper into the interior ($m(L)$ increases), thereby increasing \dim_{eff} .*
- (ii) *The μ operator does not change the realizability class or margin, and therefore leaves $\mathcal{D}(m(L), \bar{\rho}, \mathcal{R})$ invariant. It is DOF-inert within the tested regime.*

Proof sketch. Part (i): The Phase Mapping corpus shows that α deformation can change the realizability class (e.g., ^{28}Si transitions from HARD to Full as α increases). Since $\mathcal{D}(m(L), \bar{\rho}, \mathcal{R})$ is monotonic in $m(L)$ (Theorem 4.1) and $m(L)$ increases with α for such near-boundary systems, new DOF become accessible. Part (ii): The μ -column corpus (127 runs, 8 systems) shows zero class changes and constant $m(L)$ under μ deformation within the tested range $[0.80, 1.20]$, hence \mathcal{D} is invariant. \square \square

9.2 Operator Regime Behaviour and Structural Attractors

Theorem 9.1 establishes that \hat{O}_α can activate new DOF in near-boundary systems. The extended corpus — spanning atomic Zeeman ladders, cosmological distance ladders, condensed matter gap structures, and crystallographic distance spectra across 35 systems — reveals that this activation takes qualitatively distinct forms depending on the structural domain. We formalise these distinctions here.

Definition 9.2 (Operator Regime Behaviour). Let \hat{O}_α be the structural deformation operator acting on an admissible ladder L . The *operator regime behaviour* is the qualitative mode of evolution of $\mathcal{D}(m(L), \bar{\rho}, \mathcal{R})$ and $\dim_{\text{eff}}(L)$ under deformation:

$$\mathcal{D}(m(L), \bar{\rho}, \mathcal{R}) \xrightarrow{\hat{O}_\alpha} \mathcal{D}(m(L)', \bar{\rho}', \mathcal{R}').$$

The regime behaviour is *discrete*, *convergent*, or *inert* according to Definition 9.2 and classified by Theorem 9.2 below.

Theorem 9.2 (Operator Regime Classification). *Under admissible deformation by \hat{O}_α , structural systems exhibit one of three distinct operator regimes:*

- (i) **Discrete Activation Regime.** *There exist systems for which $m(L) \approx 0$ transitions to $m(L)' \gg 0$ under finite deformation, producing a discontinuous increase in $\dim_{\text{eff}}(L)$. This corresponds to stepwise crossing of DOF activation thresholds $m_{\min}(\delta, \bar{\rho}, \mathcal{R})$.*
- (ii) **Continuous Convergence Regime.** *There exist systems for which $m(L) \rightarrow m^* > 0$ continuously under deformation, with $\dim_{\text{eff}}(L) \rightarrow \dim^*$ smoothly. This corresponds to monotone contraction of the accessible DOF set toward a stable structural manifold.*
- (iii) **Inert Regime.** *There exist systems for which $m(L)' = m(L)$ and $\mathcal{D}(L') = \mathcal{D}(L)$ throughout the deformation domain. The operator activates no new structural directions; DOF and margin are deformation-invariant.*

Proof sketch. The three regimes exhaust all qualitative behaviours of $m(L)$ under bounded admissible deformation. The discrete regime follows from the threshold structure of Definition 4.1: if $m(L)$ crosses a threshold $m_{\min}(\delta)$, the DOF set \mathcal{D} gains the corresponding axis discontinuously. The convergence regime follows from the monotonicity of \mathcal{D} in $m(L)$ (Theorem 4.1) when $m(L)$ evolves continuously toward a limiting value m^* . The inert regime corresponds to systems for which \hat{O}_α does not change $m(L)$ or \mathcal{R} within the tested domain — the margin remains stationary and no threshold is crossed. Empirically: atomic Zeeman systems (e.g. gold, helium singlet) exhibit the discrete regime; crystallographic distance ladders exhibit the convergence regime; cosmological radial and redshift ladders exhibit the inert regime. \square \square

Remark 4. The operator \hat{O}_α is not universally active: its regime-dependence is itself a structural observable. A system’s operator regime is determined by its initial structural state $(m(L), \mathcal{R})$ and the distance to the nearest activation threshold. This extends Theorem 9.1 from a binary (active/inert) to a three-class classification.

Definition 9.3 (Structural Attractor). A *structural attractor* is a region (m^*, \dim^*) in the $(m(L), \dim_{\text{eff}})$ phase space such that, under repeated application of \hat{O}_α :

$$\hat{O}_\alpha^k(L) \longrightarrow L^* \quad \text{as } k \rightarrow \infty,$$

with $m(L^*) = m^*$ and $\dim_{\text{eff}}(L^*) = \dim^*$, independently of the initial ladder L within a given structural class.

Theorem 9.3 (Existence of Domain-Specific Structural Attractors). *For systems in the continuous convergence regime (Theorem 9.2(ii)), there exists an empirically observed stable attractor (m^*, \dim^*) such that:*

$$\lim_{k \rightarrow \infty} \dim_{\text{eff}}(\hat{O}_\alpha^k(L)) = \dim^*, \quad \lim_{k \rightarrow \infty} m(\hat{O}_\alpha^k(L)) = m^* > 0,$$

for all ladders L in the basin of attraction. Attractors are domain-specific: the converged values (m^*, \dim^*) depend on the structural class of the domain rather than on individual ladder properties. We conjecture uniqueness of the attractor within each structural domain; a proof would require establishing global stability of the fixed-point map, which is beyond the current corpus.

Proof sketch. From Theorem 4.1, \mathcal{D} is monotone non-decreasing in $m(L)$. In the convergence regime, $m(L)$ evolves toward a limit m^* set by the structure of the deformation operator and the boundary geometry of \mathcal{M}_{adm} . Since \mathcal{D} is finite (finitely many admissible axes exceed the threshold at m^*), \dim_{eff} stabilises at $\dim^* = |\mathcal{D}(m^*, \bar{\rho}^*, \mathcal{R}^*)|$. The domain-specificity of the attractor follows from the fact that the threshold profile $\{m_{\text{min}}(\delta)\}$ depends on the realizability class \mathcal{R} , which differs between structural domains. Empirically: the crystallographic corpus (19 systems across 7 chemical families) converges to $\alpha \in [1.34, 1.47]$ and $m^* \in [0.553, 0.597]$ at $\dim^* = 3$, independently of initial α values spanning $[0.37, 6.01]$. □ □

Corollary 9.1 (Dimensional Attractor Collapse). *If a structural attractor exists for a given domain, then there exists \dim^* such that $\dim_{\text{eff}}(L) \rightarrow \dim^*$ for all ladders in the basin of attraction. The system forgets its initial DOF configuration and collapses onto the attractor’s stable dimensional state.*

Theorem 9.4 (Universal Margin Band Convergence). *There exists a bounded interval $[m_1, m_2]$ with $m_1 > 0$ such that, across the tested domains (atomic, cosmological, condensed matter, crystallographic), admissible deformation drives systems toward $m^* \in [m_1, m_2]$:*

$$\lim_{k \rightarrow \infty} m(\hat{O}_\alpha^k(L)) \in [m_1, m_2].$$

The corpus-supported estimate is $[m_1, m_2] \approx [0.553, 0.600]$, observed across 35 systems spanning atomic spectra, cosmic web surveys, condensed matter gap structures, and crystallographic distance ladders.

Proof sketch. The universal character of $[m_1, m_2]$ follows from the cross-domain convergence of $m(L)$ under \hat{O}_α : all systems in the continuous convergence regime stabilise within this band regardless of physical domain or initial conditions. Systems in the inert regime (cosmological domain) are already positioned within or near $[m_1, m_2]$ at zero deformation. Systems in the discrete regime (atomic domain) enter $[m_1, m_2]$ after threshold crossing. The band thus functions as a *structural fixed point region* of the deformation dynamics, not merely an empirical overlap. \square \square

Theorem 9.5 (Operator-Regime-DOF Correspondence). *Each operator regime corresponds to a distinct DOF evolution pattern and dimensional outcome:*

<i>Regime</i>	<i>DOF behaviour</i>	<i>Dimensional effect</i>
<i>Discrete</i>	<i>threshold activation</i>	<i>discontinuous jump in \dim_{eff}</i>
<i>Continuous convergence</i>	<i>contraction to attractor</i>	$\dim_{\text{eff}} \rightarrow \dim^*$
<i>Inert</i>	<i>no activation</i>	$\dim_{\text{eff}} = \text{constant}$

This correspondence extends Theorem 9.1: the action of \hat{O}_α is not uniform but regime-dependent, producing activation, convergence, or invariance according to the initial structural state.

Proof sketch. Follows directly from Theorem 9.2 combined with the threshold characterisation of Definition 4.1: discrete regime produces threshold crossings (jumps in \mathcal{D}); convergence regime produces smooth approach to m^* (gradual stabilisation of \mathcal{D}); inert regime produces no threshold crossings (invariant \mathcal{D}). \square \square

9.3 Spectral Invariance and Encoding Collapse

The preceding subsections establish how the deformation operator acts on gap-derived structural coordinates $(\alpha_{\text{gs}}, m(L), \dim_{\text{eff}})$. We now show that the level-derived coordinate γ is orthogonal to this deformation space, and that the operator acts as a canonical representation selector: different ladder encodings of the same physical system collapse toward the same structural attractor under admissible deformation. Together, these results complete the four-coordinate description of the UNNS structural phase space.

Definition 9.4 (Spectral Growth Exponent). Let $L = (x_1 \leq x_2 \leq \dots \leq x_n)$ be an admissible ladder. The *spectral growth exponent* $\gamma(L)$ is the power-law slope of the ordered level sequence:

$$\gamma(L) = \left. \frac{d \log x_i}{d \log i} \right|_{\text{OLS}},$$

computed by ordinary least squares on $\{(\log i, \log x_i)\}_{i:x_i>0}$. The spectral growth exponent is derived from the level values $\{x_i\}$ directly, not from the gap sequence $\{\Delta_i\}$, and therefore measures the asymptotic growth law of the underlying spectrum independently of its internal gap structure.

Remark 5 (Coordinate Separation). The structural coordinates of an admissible ladder fall into two independent groups:

Coordinate	Source	Deformation dependence
α_{gs}	gap sequence $\{\Delta_i\}$	deformable (changes with B)
$m(L)$	gap sequence $\{\Delta_i\}$	convergent (drives toward m^*)
dim_{eff}	gap covariance structure	discrete (threshold jumps)
γ	level sequence $\{x_i\}$	invariant (see Theorem 9.6)

The first three coordinates are gap-derived; the fourth is level-derived. This separation underlies the orthogonality established in Theorem 9.6.

Theorem 9.6 (Spectral Invariance under Admissible Deformation). *Let $L(B)$ be a ladder evolving under the admissible deformation operator \hat{O}_B , and let $\gamma(L)$ be the spectral growth exponent (Definition 9.4). If \hat{O}_B acts only on gap structure — that is, it modifies the gap sequence $\{\Delta_i\}$ without altering the level-generating law — then:*

$$\gamma(L(B)) = \gamma(L(0)) \quad \text{for all admissible } B.$$

Proof sketch. The spectral growth exponent $\gamma(L)$ is a functional of $\{x_i\}$, not of $\{\Delta_i\}$. Under an admissible deformation that modifies gaps $\Delta_i \mapsto \Delta'_i$ without changing the level-generating law (e.g., $x_i = -R/i^2$ for hydrogenic levels, or $x_i = d_i$ for pairwise distances under a fixed lattice structure), the level values satisfy $x_i(B) = x_1 + \sum_{j < i} \Delta_j(B)$. If the deformation is level-law-preserving, the leading-order power-law growth $x_i \sim i^\gamma$ is governed by the level-generating law and not by the specific gap perturbation. Formally, let $x_i(B) = f(i) + g(\Delta(B), i)$ where f encodes the generating law and g encodes gap perturbation contributions. If $g = o(f)$ asymptotically, then $\gamma(L(B)) = \gamma(L(0))$ to leading order. The condition is satisfied whenever the deformation is bounded ($B \in [0, 1]$) and the spectral growth is power-law dominated.

Empirically: across 19 crystallographic systems, $|\Delta\gamma/\Delta B| < 0.01$ over $B \in [0, 1]$ with $\gamma \in [0.317, 0.345]$ (s.d. 0.008). In the atomic corpus, helium singlet maintains $\gamma = 0.00350$ while dim_{eff} jumps by 2 and $m(L)$ increases by 0.42. The γ -invariance holds across both the discrete and convergence regimes, confirming that gap-structure deformation does not reach the level-generating law. □ □

Corollary 9.2 (Four-Coordinate Structural Phase Space). *The structural state of an admissible ladder under deformation is completely described by the four-tuple $(\alpha_{\text{gs}}, m(L), \text{dim}_{\text{eff}}, \gamma)$, with dynamics:*

- α_{gs} — deformable: changes continuously under \hat{O}_B ;
- $m(L)$ — convergent: driven toward a domain-specific attractor m^* ;
- dim_{eff} — discrete: jumps at activation thresholds, otherwise constant;
- γ — invariant: preserved by all level-law-preserving deformations.

The phase space is therefore four-dimensional with mixed dynamics: three active coordinates and one structural invariant. The admissibility manifold \mathcal{M}_{adm} is parameterised by $(\alpha_{\text{gs}}, m(L), \text{dim}_{\text{eff}})$; γ provides an orthogonal invariant axis stratifying \mathcal{M}_{adm} into iso- γ sheets. Systems on distinct γ -sheets cannot be related by level-law-preserving deformation, making γ a structural conservation law of the deformation dynamics within each physical domain.

Theorem 9.7 (γ -Stratification of the Admissibility Manifold). *The admissibility manifold \mathcal{M}_{adm} decomposes into disjoint invariant sectors under level-law-preserving admissible deformation:*

$$\mathcal{M}_{\text{adm}} = \bigsqcup_{\gamma} \mathcal{M}_{\gamma}, \quad \mathcal{M}_{\gamma} := \{L \in \mathcal{M}_{\text{adm}} : \gamma(L) = \gamma\},$$

where the union is taken over all attained values of γ . No level-law-preserving admissible deformation maps a ladder from \mathcal{M}_{γ_1} to \mathcal{M}_{γ_2} when $\gamma_1 \neq \gamma_2$. Therefore γ is not merely an invariant observable but a stratifying coordinate of the structural phase space: it partitions \mathcal{M}_{adm} into dynamically disconnected sectors.

Proof sketch. By Theorem 9.6, $\gamma(L(B)) = \gamma(L(0))$ for all admissible trajectories that preserve the level-generating law. Hence every admissible trajectory remains on a fixed- γ sheet: $L(B) \in \mathcal{M}_{\gamma(L(0))}$ for all B . The sectors \mathcal{M}_{γ} are therefore forward-invariant under the deformation dynamics. Since distinct values of γ define disjoint sectors by definition, no trajectory can cross between sectors. This upgrades the coordinate separation of Corollary 9.2 from orthogonality to manifold stratification: γ does not merely parametrise an invariant axis — it defines globally disconnected submanifolds of \mathcal{M}_{adm} . \square \square

Corollary 9.3 (Dynamic Non-Reachability Across γ -Sectors). *If two admissible ladders satisfy $\gamma(L_1) \neq \gamma(L_2)$, then no finite sequence of level-law-preserving admissible deformations connects L_1 to L_2 . The two systems may share identical values of $(\alpha_{\text{gs}}, m(L), \text{dim}_{\text{eff}})$ and yet remain structurally distinct by spectral sector. In particular, encoding collapse (Theorem 9.8) cannot move a system between γ -sectors: all encodings of the same physical system must carry the same γ for the collapse to a shared attractor (Theorem 9.8) to be consistent with the stratification of Theorem 9.7.*

Theorem 9.8 (Encoding Collapse under Admissible Deformation). *Let a physical system S admit a finite set of admissible encodings $\{L_1, L_2, \dots, L_n\} \subset \mathcal{E}(S)$, with initial structural parameters $(\alpha_{\text{gs}}^{(i)}, m(L_i), \text{dim}_{\text{eff}}(L_i))$ varying across encodings. If each L_i lies in the continuous convergence regime (Theorem 9.2(ii)), then under admissible deformation:*

$$(\alpha_{\text{gs}}^{(i)}(B), m(L_i(B)), \text{dim}_{\text{eff}}(L_i(B))) \longrightarrow (\alpha_{\text{gs}}^*, m^*, \text{dim}^*) \quad \text{as } B \rightarrow B_{\text{max}},$$

independently of i . That is, distinct encodings of the same system collapse to the same structural attractor.

Proof sketch. By Theorem 9.3, each L_i in the continuous convergence regime has a domain-specific attractor (m^*, dim^*) determined by the realizability class \mathcal{R} of the domain, not by the individual ladder. Since all encodings $\{L_i\}$ are encodings of the same physical system S within the same structural domain, they share the same realizability class and hence the same attractor. The α_{gs}^* convergence follows from the deformation dynamics: the operator \hat{O}_B reorganises the gap structure toward the canonical gap scaling regime of the domain, erasing the initial encoding-dependent spread. Empirically: the crystallographic corpus shows $\alpha_{\text{gs}}^{(i)}(0) \in [0.37, 6.01]$ collapsing to $\alpha_{\text{gs}}^* \in [1.34, 1.47]$ (s.d. 0.04), with simultaneous m -convergence to $m^* \in [0.553, 0.597]$ and $\text{dim}_{\text{eff}} \rightarrow 3$, across 7 chemical families and 19 systems. \square \square

Remark 6 (Encoding Collapse as Canonical Selection). Theorem 9.8 provides a dynamical interpretation of the Maximum-Margin Principle (Interaction Unification, Definition 11.1): among all admissible encodings, the deformation operator selects the canonical one by driving all encodings toward the same structural attractor. The attractor coordinates $(\alpha_{\text{gs}}^*, m^*, \text{dim}^*)$ constitute the canonical structural representation of the physical system under the given domain's realizability class. Different encodings are different projections of the same underlying structure; the operator acts as a representation eraser and canonical structure selector simultaneously.

Principle 2 (Maximum-Margin Direction of Encoding Collapse). *Let S be a physical system with admissible encoding family $\mathcal{E}(S) = \{L_i\}$. If the family lies in the continuous convergence regime (Theorem 9.2(ii)), then the operator-induced encoding collapse is not neutral convergence but is directed toward the canonical representation selected by maximal admissible margin:*

$$L_{\text{can}} = \arg \max_{L \in \mathcal{E}(S)} m(L).$$

The deformation operator preferentially erases encoding-dependent structural spread by driving all encodings toward the maximum-margin representative of the encoding class. The attractor $(\alpha_{\text{gs}}^, m^*, \text{dim}^*)$ is the structural image of the Maximum-Margin Principle under admissible deformation: the canonical endpoint of an optimisation in margin, not merely a convenient convergence point. This elevates the Interaction Unification's static selection criterion (Definition 11.1) to a dynamical law: encoding collapse is maximum-margin selection.*

Corollary 9.4 (Canonical Attractor Identification). *If an encoding family $\mathcal{E}(S)$ converges to a shared attractor $(\alpha_{\text{gs}}^*, m^*, \text{dim}^*)$ under admissible deformation, then:*

- (i) *The attractor represents the canonical encoding class of S within the tested structural domain.*
- (ii) *m^* is the terminal margin of canonicalisation: the margin value at which the maximum-margin selection process stabilises.*
- (iii) *The attractor coordinates $(\alpha_{\text{gs}}^*, m^*, \text{dim}^*)$ are the dynamical image of the Maximum-Margin Principle: they are the structural coordinates of L_{can} as determined by the deformation operator.*

Theorem 9.9 (α_{gs} -Convergence Dynamics). *In the continuous convergence regime, the gap scaling exponent $\alpha_{\text{gs}}(B)$ satisfies an exponential approach to the domain attractor α_{gs}^* :*

$$\alpha_{\text{gs}}(B) - \alpha_{\text{gs}}^* \sim (\alpha_{\text{gs}}(0) - \alpha_{\text{gs}}^*) e^{-kB}, \quad k > 0,$$

for some domain-dependent rate constant k . Convergence is effectively complete by $B \lesssim 2/k$.

Proof sketch. The deformation operator applies a scale-and-shape transformation to the gap sequence at each step. Linearising around the attractor: if $\alpha_{\text{gs}} - \alpha_{\text{gs}}^*$ is small, the restoring force is proportional to the displacement (since the attractor is a fixed point of the gap-reorganisation map), giving exponential relaxation with rate k determined by the local

slope of the map near the attractor. The condition $k > 0$ follows from the stability of the attractor (Theorem 9.3): a repulsive fixed point would contradict convergence. Empirically: KNbO_3 trigonal decays from $\alpha_{\text{gs}} = 6.007$ to $\alpha_{\text{gs}} \approx 1.27$ by $B = 0.10$, implying $k \approx \ln(4.7/\delta)/0.10$ where δ is the residual at $B=0.1$; all 19 systems complete convergence before $B = 0.20$, bounding $k \gtrsim 10$. \square \square

Principle 3 (Spectral Invariance as Structural Conservation). *The spectral growth exponent γ is a structural conservation law of admissible deformation: it is preserved by \hat{O}_B whenever the deformation is level-law-preserving. As a consequence:*

- (i) *Physical systems with distinct γ are structurally non-equivalent under level-law-preserving deformation: no sequence of admissible operations connects them.*
- (ii) *The pair (γ, m^*) jointly classifies the structural domain of a physical system: γ identifies the spectral family; m^* identifies its position within the admissibility manifold.*
- (iii) *The full four-coordinate system $(\alpha_{\text{gs}}, m(L), \dim_{\text{eff}}, \gamma)$ provides a complete structural description with minimal redundancy: no two coordinates are derivable from the others within the UNNS framework.*

Remark 7 (Four-Coordinate Structural Phase Space — Synthesis). The structural phase space of admissible ladders is a four-coordinate system $(\alpha_{\text{gs}}, m(L), \dim_{\text{eff}}, \gamma)$ with mixed dynamics: continuous $(\alpha_{\text{gs}}, m(L))$, discrete (\dim_{eff}) , and invariant (γ) . The admissibility manifold is partitioned into dynamically disconnected spectral sectors \mathcal{M}_γ (Theorem 9.7); within each sector, the deformation operator \hat{O}_B drives structural states toward domain-specific fixed points (m^*, \dim^*) governed by regime-dependent flows (Theorems 9.3–9.9). The spectral invariant γ is preserved throughout, functioning as a structural conservation law of the dynamics (Principle 3).

Theorem 9.10 (Regime-Local Attractor). *Let \mathcal{R}_{int} denote an interaction regime in the sense of Section 8 and the companion Interaction Unification manuscript. Suppose the tested corpus samples only ladders whose margins lie within a single regime band \mathcal{R}_{int} . Then any empirically observed attractor band $m^* \in [m_1, m_2]$ derived from that corpus is a regime-local fixed-point region of the deformation dynamics within \mathcal{R}_{int} , and does not constitute evidence of cross-regime universality. In particular, since all 35 systems in the present corpus satisfy $m(L) \in [0.50, 1.00]$ (strong-like regime), the attractor band of Theorem 9.4 belongs to the strong-like regime only. No conclusion follows about fixed-point bands in the EM-like ($m(L) \sim 10^{-2}$), weak-like ($m(L) \sim 10^{-3}$), or gravity-like ($m(L) \sim 10^{-4}$) regimes without corresponding corpus coverage.*

Proof sketch. Theorem 9.4 is a corpus-supported result: its proof sketch cites convergence data from 35 systems that, by Section 11.1 (encoding scope paragraph), all lie within the strong-like interaction regime. The empirical attractor therefore inherits the scope of the corpus: it is a fixed point of the deformation dynamics within the strong-like regime band, not a claim about all possible margin values. Any extension to other regime bands requires new corpus evidence drawn from those bands specifically. \square \square

Corollary 9.5 (Conditional Universality of the Margin Band). *The attractor band $m^* \in [0.553, 0.600]$ (Theorem 9.4) may be called universal only in the restricted sense: universal-ity within the strong-like corpus currently tested, not universality across all interaction*

regimes. Whether analogous fixed-point bands $[m'_1, m'_2]$ exist in EM-like, weak-like, or gravity-like regimes is an open empirical question. If such bands exist and differ from $[0.553, 0.600]$, the margin-band result of Theorem 9.4 generalises to a regime-indexed family of local attractors; if they coincide, a stronger cross-regime universality claim becomes available.

10 The Dimensional Selection Principle

Principle 4 (Dimensional Selection Principle). *Only degree-of-freedom sets \mathcal{D} that are compatible with:*

- (i) *the admissibility constraint (USL),*
- (ii) *the realizability classification (PRP),*
- (iii) *the connectivity margin $m(L) > 0$ (or $m(L) \rightarrow 0^+$ for gravity),*

are physically instantiated. Equivalently: not all dimensions are possible; only those that can be realised as admissible structural transformation axes under the margin constraints of the system.

Theorem 10.1 (Dimensional Collapse at Boundary). *If $m(L) \rightarrow 0$, then:*

$$\dim_{\text{eff}}(L) \rightarrow \dim_{\text{boundary}},$$

where \dim_{boundary} corresponds to the dimension of the tangent subspace of the realizability boundary. At the boundary itself ($m(L) = 0$), only axes with $m_{\min} = 0$ remain accessible, which are precisely those tangent to the boundary.

Proof sketch. By Definition 4.1, a direction δ is accessible iff $m(L) \geq m_{\min}(\delta, \bar{\rho}, \mathcal{R})$. As $m(L) \rightarrow 0$, only directions with $m_{\min} = 0$ satisfy the inequality. These correspond to the tangent subspace of the realizability boundary. Hence \dim_{eff} collapses to the dimension of that subspace. □ □

Corollary 10.1 (Absence of Arbitrary Dimensionality). *The Dimensional Selection Principle implies that there is no physical configuration corresponding to an arbitrarily chosen dimensionality. The observed dimensionality of a system is fixed by its structural state and cannot be varied independently without crossing a realizability boundary.*

11 Empirical Alignment with Corpus Results

The dimensionality framework is consistent with — and in fact predicted by — the existing UNNS corpus. Theorems 9.2–9.10 are empirically grounded structural theorems: their statements are derived from the formal framework, but their validity is established through corpus-wide observational consistency across 35 systems and 4 physical domains. Where a theorem rests primarily on corpus evidence rather than deductive proof, this is marked “corpus-supported” in Table 1.

Theorem 11.1 (Dimensional Rigidity under Bounded Deformation). *For any admissible ladder L and deformation domain Ω_L where realizability class is invariant (Principle 1), we have:*

$$\dim_{\text{eff}}(L) = \text{constant over } \Omega_L.$$

This follows from zero inter-class transitions across 22,817 evaluations in the Phase Mapping corpus: since $\mathcal{C}(L)$ and $m(L)$ are invariant over Ω_L , the threshold condition $m(L) \geq m_{\min}(\delta, \bar{\rho}, \mathcal{R})$ is unchanged, hence \mathcal{D} is invariant.

Example 1 (α -Driven DOF Activation in Silicon). Consider silicon-28 in the nuclear constants deformation corpus:

- **Initial state** ($\alpha = 0.90$): HARD class, $m(L) \approx 0$. Effective dimensionality is minimal ($\dim_{\text{eff}} \approx \dim_{\text{boundary}}$).
- **Apply α deformation**: Increase α to 1.00.
- **Final state** ($\alpha = 1.00$): FULL class, $m(L) \gg 0$. New DOF become accessible as m_{\min} thresholds are crossed.
- **Conclusion**: \dim_{eff} increases discontinuously at the class transition boundary.

This demonstrates that α activates new degrees of freedom in near-boundary systems, consistent with Theorem 9.1.

Additional alignments:

1. **Universal structural rigidity** (Phase Mapping corpus): Zero inter-class transitions across 22,817 evaluations implies that \dim_{eff} is constant within each ladder construction under (α, μ) deformation. This is Theorem 11.1.
2. **Zero structural commutators**: $C(\alpha, \mu; L) = 0$ implies that the order of operator application does not affect the active DOF set — commutativity of DOF activation.
3. **Representation dependence**: Different ladder constructions of the same physical system yield different realizability classes, hence different \dim_{eff} . The canonical ladder problem (maximum margin) selects the encoding that maximises accessible DOF.
4. **Interaction classification**: The four interaction regimes correspond to distinct DOF activation profiles (Section 8), consistent with the asymptotic classification of Φ .
5. **Operator separation**: α can activate DOF in near-boundary systems; μ is inert within the tested regime. This matches the corpus finding that α is structurally active while μ is inert.
6. **Operator regime classification** (Theorem 9.2): The extended corpus (35 systems across four domains) supports the three-regime classification. Atomic Zeeman systems (Au, He singlet, Fe $\text{Fm}\bar{3}\text{m}$) exhibit discrete activation: \dim_{eff} jumps at the first non-zero deformation step. Crystallographic distance ladders (19 systems, 7 chemical

families) exhibit continuous convergence: α values spanning $[0.37, 6.01]$ at $B=0$ all contract to $[1.34, 1.47]$ at $B=1$. Cosmological ladders (2MRS, DESI, SDSS) exhibit the inert regime: $m(L)$ and dim_{eff} are invariant across the full deformation sweep.

7. **Universal margin band** (Theorem 9.4): Across all four domains, admissible deformation drives $m(L) \rightarrow [0.553, 0.600]$. This band is occupied at zero field by cosmological systems, entered after threshold crossings by atomic systems, and converged toward by crystallographic systems under operator action. The band functions as the structural fixed-point region of the deformation dynamics, consistent with the universal margin convergence claim of Theorem 9.4.

11.1 Multi-Domain Corpus Results and Theorem Correspondence

We present a systematic mapping from the four-domain scaling corpus (35 systems: 6 atomic Zeeman, 5 cosmological, 5 condensed matter, 19 crystallographic; see Section 9.2 for corpus description) to the theorems of this manuscript and the companion Interaction Unification paper. The purpose is to make the derivation chain from raw data to formal statement explicit and independently verifiable: each corpus result is traceable to a specific theorem, and each theorem is grounded in a corpus observation.

Remark 8 (Notation). Throughout Section 11.1, the symbol α_{gs} denotes the *gap scaling exponent* extracted by the pipeline (the power-law slope of the sorted gap sequence), to distinguish it from the structural deformation parameter α used elsewhere in this manuscript and in the companion papers.

Table 1: Mapping from four-domain corpus results to formal theorems. “Established” denotes results derived from definitions and prior principles without additional corpus dependence. “Corpus-supported” denotes results whose proof sketch appeals to observed data in the extended corpus (35 systems, 4 domains). [†]The 2MRS result corresponds to the *inverse* of Theorem 10.1: maximal margin ($m(L) = 1$) with uniform gap spacing produces $\text{dim} = 1$ because perfect gap uniformity eliminates covariance variance, collapsing the accessible DOF set to a single axis. This is not a boundary collapse but a crystallised-interior state.

Corpus result	Systems	Theorem / Principle	Status
Zero dim_{eff} transitions across 22,817 evaluations at $(\alpha, \mu) \in [0.80, 1.20]^2$	Phase Mapping corpus	Theorem 11.1 (Dim. Rigidity)	established
Discrete dim_{eff} jump at $B=0.01$: Au +1, He singlet +2, Fe $\text{Fm}\bar{3}m$ +2	3 atomic systems	Theorem 9.2(i) (Discrete Activation)	corpus-supported

(Table 1 continued)

Corpus result	Systems	Theorem / Principle	Status
α_{gs} converges to [1.34, 1.47] from [0.37, 6.01] for 19 crystal systems	Crystallographic corpus	Theorems 9.2(ii), 9.3 (Convergence; Attractor)	corpus-supported
Cosmological ladders: $\Delta m(L)/\Delta B \approx 0$, \dim_{eff} frozen throughout	5 cosmo. ladders	Theorem 9.2(iii) (Inert Regime)	corpus-supported
$m(L) \rightarrow [0.553, 0.600]$ across all four domains at $B=1$	35 systems	Theorem 9.4 (Universal Margin Band)	corpus-supported
$\dim_{\text{eff}} \in \{1, 2, 3\}$ exclusively; no intermediate values observed	All 35 systems	Principle 4 (Dimensional Selection)	established
Fe $\text{Im}\bar{3}\text{m}$ (bcc) $\dim=3$; Fe $\text{Fm}\bar{3}\text{m}$ (fcc) $\dim=1$ at $B=0$	2 Fe polymorphs	Theorem 5.1(ii) (Regime Dependence)	corpus-supported
BaTiO_3 cubic and rhombohedral: same element, different $\alpha_{\text{gs}}, m(L)$	4 BaTiO_3 phases	Theorem 5.1(iii) (Structural Determinacy)	corpus-supported
\dim_{eff} increases monotonically from $\dim=1$ (boundary) to $\dim=3$ (interior)	Cross-domain	Theorem 4.1 (Monotonicity of DOF)	established
\dim_{eff} post-transition locked at $\dim=3$ for all three transitioning systems	Au, He, Fe fcc	Corollary 9.1 (Dim. Attractor Collapse)	corpus-supported
All 35 systems produce $m(L) \in [0.50, 1.00]$; no system reaches weak or gravity band	All 35 systems	Interaction Unif. Table 1 (scope: strong-like regime only)	corpus-supported
2MRS radial: $m(L) = 1.000$, $\dim=1$ (uniform gap sequence, maximally ordered)	1 cosmo. system	Theorem 10.1 (Dim. Collapse, inverse) [†]	corpus-supported
Operator response modes and interaction regimes are orthogonal classifications	Cross-domain	Theorem 9.5 + IU Def. 3.1	established
γ invariant under full B -sweep: crystals $ \Delta\gamma < 0.01$; He singlet $\gamma = 0.00350$ constant while \dim_{eff} jumps by 2	19 crystal + 1 atomic	Theorem 9.6 (Spectral Invariance)	corpus-supported
Different encodings of same domain collapse to same $(\alpha_{\text{gs}}^*, m^*, \dim_{\text{eff}}^*)$	19 crystal (7 families)	Theorem 9.8 (Encoding Collapse)	corpus-supported
Systems with distinct γ cannot be connected by admissible deformation	Cross-domain	Theorem 9.7 + Corollary 9.3	established

(Table 1 continued)

Corpus result	Systems	Theorem / Principle	Status
Collapse is directed toward max-margin representative, not neutral convergence	Crystal corpus	Principle 2 + Corollary 9.4	corpus-supported
Attractor band [0.553, 0.600] is within strong-like regime only	All 35 systems	Theorem 9.10 + Corollary 9.5	established

Discrete activation regime: corpus instances. Three systems exhibit the discrete operator response regime (Theorem 9.2(i)). Gold at $B=0$: ($\alpha_{\text{gs}} = -1.478$, $m(L) = 0.520$, $\text{dim}_{\text{eff}} = 2$); at $B=0.01$: ($\alpha_{\text{gs}} = -0.240$, $m(L) = 0.859$, $\text{dim}_{\text{eff}} = 3$). Helium singlet at $B=0$: ($\alpha_{\text{gs}} = -1.670$, $m(L) = 0.580$, $\text{dim}_{\text{eff}} = 1$); at $B=0.01$: ($\alpha_{\text{gs}} = -0.070$, $m(L) = 1.000$, $\text{dim}_{\text{eff}} = 3$). Iron $\text{Fm}\bar{3}\text{m}$ at $B=0$: ($\alpha_{\text{gs}} = 0.372$, $m(L) = 0.841$, $\text{dim}_{\text{eff}} = 1$); at $B=0.01$: ($\alpha_{\text{gs}} = 1.483$, $m(L) = 0.553$, $\text{dim}_{\text{eff}} = 3$). In all three cases the transition occurs at the first non-zero field step $B=0.01$, the margin shifts by $\Delta m(L) \geq 0.33$, and dim_{eff} locks at the post-transition value for all remaining field steps. Each instance is consistent with Corollary 9.1: the system enters the attractor basin and does not return.

Continuous convergence regime: crystallographic attractor. The crystallographic corpus provides 19 systems from 7 chemical families (Al_2O_3 , BaTiO_3 , Fe, KNbO_3 , SiO_2 , TiPbO_3 , ZrO_2). At $B=0$, gap scaling exponents span $\alpha_{\text{gs}} \in [0.37, 6.01]$. At $B=1$, all 19 systems converge to $\alpha_{\text{gs}} \in [1.34, 1.47]$ (mean 1.39, s.d. 0.04) and $m(L) \in [0.553, 0.597]$ at $\text{dim}_{\text{eff}} = 3$. This convergence is domain-specific (Theorem 9.3): the attractor coordinates ($m^* \approx 0.578$, $\text{dim}^* = 3$) are the same across all seven families despite their different space groups, lattice constants, and initial conditions. The spectral growth exponent γ — computed from energy levels rather than gaps — is invariant under the sweep for all 19 systems: $\gamma \in [0.317, 0.345]$ at all B . This γ -invariance is not yet covered by any theorem in this manuscript and constitutes an open empirical observation; see Open Problem 7 below.

Inert regime: cosmological corpus. Five cosmological ladders (2MRS radial, DESI synthetic, DESI xyz, DESI redshift, SDSS CW2) show $\Delta m(L)/\Delta B < 10^{-10}$ and constant dim_{eff} across the full sweep $B \in [0, 1]$. These ladders sit at $m(L) \in [0.577, 1.000]$, placing them within the strong-like interaction regime of the companion Interaction Unification manuscript (Table 1: strong-like $m(L) \sim 0.5$ –1). The cosmological ladder encoding used here — radial comoving distances and redshift catalogs — differs from the CMB power spectrum encoding used in the Interaction Unification micro-tests (Planck: $m(L) \approx 2 \times 10^{-4}$, gravity-like regime). The encoding dependence caveat of the Interaction Unification manuscript (Section 11) therefore applies: the inert operator response is a property of the specific ladder encoding, not of the cosmological interaction regime per se. The canonical interaction regime for cosmological systems requires the maximum-margin principle to select among admissible encodings.

Encoding scope and interaction regime. All 35 corpus systems produce $m(L) \in [0.50, 1.00]$, placing the entire corpus within the strong-like interaction regime of the In-

teraction Unification framework. The EM, weak, and gravity interaction regimes require $m(L) \sim 10^{-2}, 10^{-3}, 10^{-4}$ respectively — outside the range of the present corpus. The universal margin band $[m_1, m_2] \approx [0.553, 0.600]$ (Theorem 9.4) is therefore a within-strong-regime structural fixed point, not a cross-interaction-regime phenomenon. Whether analogous attractors exist within the EM, weak, and gravity regimes under appropriate encodings is an open problem.

Open observations not yet covered by theorem. Two empirical regularities in the corpus are robust but lack formal theorem status in the current manuscript:

- (O1) **γ -invariance and stratification:** The spectral growth exponent γ is invariant under the deformation operator \hat{O}_B across all tested systems and domains. This is now formalised by Theorem 9.6 (Spectral Invariance), Theorem 9.7 (γ -Stratification), and Corollary 9.3 (Non-Reachability). The remaining open question is whether γ -invariance persists under deformations that are *not* level-law-preserving — a class the current corpus and operator \hat{O}_B cannot probe. Determining the precise boundary of the level-law-preserving condition is the primary open problem introduced by Section 9.3.
- (O2) **Threshold universality:** The discrete activation threshold occurs at $B=0.01$ for all three transitioning systems (Au, He singlet, Fe fcc), across atomic and crystallographic domains. Whether this reflects a universal minimum deformation required to cross the nearest realizability boundary, or coincidence of the corpus construction, is undetermined.

11.2 On the Non-Derived Minimum Margin Function

A central object of the present framework is the minimum margin function $m_{\min}(\delta, \bar{\rho}, \mathcal{R})$, defined as the smallest admissible margin required for activation of a structural degree of freedom δ within a realizability class \mathcal{R} under mean structural density $\bar{\rho}$. While the existence and operational role of this function are strongly supported by the empirical corpus — manifesting through discrete dimensional transitions, attractor convergence, and regime-dependent stability bands — a closed-form derivation is not yet established. This absence is not due to conceptual incompleteness but to the current level of geometric specification of the structural state space.

Specifically, three elements remain insufficiently formalised:

- (i) **Lack of a fully metrised directional structure.** Structural directions δ are presently defined as admissible deformation axes (Definition 3.1), but are not endowed with a canonical local metric. Without such a metric, directional magnitude, curvature, and sensitivity are not uniquely specified. As a result, the notion of “minimum margin required to activate δ ” remains well-defined qualitatively — and is operationally identified through corpus transitions — but is not uniquely computable from first principles.
- (ii) **Incomplete characterisation of realizability boundaries.** The function $m_{\min}(\delta, \bar{\rho}, \mathcal{R})$ is fundamentally determined by the distance to the nearest realizability boundary

along direction δ . However, the geometry of these boundaries — while implicitly observed through threshold-crossing behaviour — has not yet been expressed as an explicit hypersurface in the structural state space. Consequently, the directional intercept defining m_{\min} cannot yet be derived analytically.

- (iii) **Absence of a differential structural response model.** Realizability classes \mathcal{R} are currently defined at a categorical level but lack a fully differential description of local structural response (e.g. Jacobian or Hessian structure) governing how admissible states evolve under infinitesimal deformation. Such a model is required to relate directional motion in δ to changes in admissibility and covariance activation, and thus to determine threshold conditions for dimensional activation.

Interpretation. The function $m_{\min}(\delta, \bar{\rho}, \mathcal{R})$ should be understood as a geometric boundary object: it represents the minimal margin at which motion along a structural direction δ remains both admissible and non-redundant within the realizability class \mathcal{R} . The empirical pipeline (UNNS Dimensional Regime Synthesis Pipeline v1) identifies this object indirectly through:

- threshold-gated dimensional transitions (discrete regime, Theorem 9.2(i));
- stabilisation of margin attractors (convergence regime, Theorem 9.3);
- selective activation of covariance modes (γ -stratification, Theorem 9.7).

These observations constrain m_{\min} only implicitly: each transition event provides a lower bound on the activation threshold along the deformation direction active at that field step, but does not determine the full threshold profile $\{m_{\min}(\delta_i)\}$.

Outlook. A closed derivation of $m_{\min}(\delta, \bar{\rho}, \mathcal{R})$ requires a refinement of the framework into a fully local geometric theory of structural state space, incorporating:

- (a) a canonical directional metric on admissible deformations,
- (b) an explicit representation of realizability boundaries as hypersurfaces in \mathcal{M}_{adm} ,
- (c) and a differential response model linking deformation to covariance activation.

Such an extension would elevate the present framework from a structurally complete regime theory to a fully differential theory of dimensional emergence.

Status. The non-derivation of m_{\min} does not limit the predictive or classificatory power of the current framework. The four-coordinate phase space $(\alpha_{\text{gs}}, m(L), \dim_{\text{eff}}, \gamma)$, the operator regime classification, and the empirical attractor results all hold independently of the explicit form of m_{\min} . Rather, this subsection delineates the next layer of formal development, building upon a system that is already empirically validated and internally consistent.

12 From Effective Dimensionality to Observable Scaling

12.1 Scaling Selection Principle

We now extend the UNNS dimensionality framework from classificatory to predictive form. The central claim is that effective dimensionality does not merely label structural regimes, but constrains the asymptotic scaling behaviour of admissible systems. Since $\dim_{\text{eff}}(L)$ counts the active structural transformation axes accessible under the current margin and realizability state, it measures the number of independent channels available for observable response.

Principle 5 (Scaling Selection Principle). *For admissible ladders, the asymptotic scaling class is selected jointly by connectivity margin $m(L)$ and effective dimensionality $\dim_{\text{eff}}(L)$. The margin determines how close the system is to a structural boundary; the effective dimensionality determines how many independent structural channels can participate in the scaling response.*

Theorem 12.1 (Scaling-Class Constraint). *Let L be an admissible ladder with structural state $(\bar{\rho}, \mathcal{R})$, connectivity margin $m(L)$, and effective dimensionality $\dim_{\text{eff}}(L)$. Then the asymptotic observable scaling class of L is constrained to a family determined by $(\dim_{\text{eff}}(L), m(L))$:*

$$\mathcal{S}_{\text{scale}}(L) \in \mathcal{F}(\dim_{\text{eff}}(L), m(L)),$$

where $\mathcal{S}_{\text{scale}}(L) \in \{\text{power law, exponential, scale-invariant, long-range weak, boundary-fragmented}\}$ is the scaling family. The functional \mathcal{F} is not assumed to be injective; distinct $(\dim_{\text{eff}}, m(L))$ may map to the same scaling family, but the family is not arbitrary — it is constrained by the pair.

Proof sketch. The scaling family is determined by the asymptotic behaviour of the interaction functional $\Phi(m(L), r, \chi(L))$ established in the Interaction Unification manuscript. The effective dimensionality $\dim_{\text{eff}}(L)$ determines the number of independent channels available for observable response, which constrains the possible asymptotic forms. The joint constraint $(\dim_{\text{eff}}, m(L))$ selects a family from the possible asymptotic classes, though not necessarily a unique one. □ □

Remark 9 (Non-degeneracy assumption). For Theorem 12.2 below, we assume that the scaling functional \mathcal{F} is not degenerate in \dim_{eff} : that is, there exist states with identical $m(L)$ but different \dim_{eff} that belong to distinct scaling families or have different exponents within the same family. This assumption is necessary for the framework to have predictive content; its falsification would require revision of the theory.

Corollary 12.1 (Exponent Variation within Class). *Systems with identical realizability class but different effective dimensionality need not share the same measurable exponents. For example, two Full-class ladders may have different \dim_{eff} and therefore different scaling exponents within the same power-law family.*

12.2 Exponent Functions and Observable Response

For a measured observable $O(r)$, we propose the following structural ansatz:

$$O(r) \sim r^{-\beta_{\text{eff}}(L)} \quad \text{or} \quad O(r) \sim e^{-r/\xi_{\text{eff}}(L)},$$

where:

$$\beta_{\text{eff}}(L) = B(\text{dim}_{\text{eff}}(L), m(L)), \quad \xi_{\text{eff}}(L) = X(\text{dim}_{\text{eff}}(L), m(L)).$$

The functions B and X are structural response functions to be determined empirically; they are not derived here. The key claim is that exponents are not arbitrary — they are constrained by $(\text{dim}_{\text{eff}}, m(L))$.

Conjecture 12.1 (Monotonic Scaling Capacity). *For fixed regime family, larger $\text{dim}_{\text{eff}}(L)$ corresponds to richer interior scaling (e.g., power-law with smaller exponent), while smaller $\text{dim}_{\text{eff}}(L)$ corresponds to reduced or boundary-dominated scaling (e.g., exponential decay or long-range weak). In the strong-like regime (deep Full), maximal dim_{eff} yields power-law scaling; in the gravity-like regime (small positive $m(L)$), minimal dim_{eff} yields long-range weak scaling.*

Theorem 12.2 (Transition Coupling). *Assume that the scaling functional \mathcal{F} is non-degenerate in dim_{eff} (Remark above). Then any deformation that changes $\text{dim}_{\text{eff}}(L)$ must induce a corresponding scaling change in at least one observable sector. Equivalently, if $\text{dim}_{\text{eff}}(L') \neq \text{dim}_{\text{eff}}(L)$, then either $\mathcal{S}_{\text{scale}}(L') \neq \mathcal{S}_{\text{scale}}(L)$ or the exponents within the same scaling family differ.*

Proof sketch. From Theorem 12.1, $\mathcal{S}_{\text{scale}}(L) \in \mathcal{F}(\text{dim}_{\text{eff}}(L), m(L))$. If dim_{eff} changes while $m(L)$ and realizability class remain unchanged, the functional dependence implies a change in $\mathcal{S}_{\text{scale}}$ or in the specific exponents unless \mathcal{F} is degenerate in dim_{eff} . By the non-degeneracy assumption, such a change occurs. □ □

12.3 Worked Example: α -Driven DOF Activation and Scaling

Using the silicon example from Section 11:

- **Initial state** ($\alpha = 0.90$): HARD class, $m(L) \approx 0$, dim_{eff} minimal. Observable scaling: fragmented, no coherent power-law; boundary-dominated response.
- **After α deformation** ($\alpha = 1.00$): FULL class, $m(L) \gg 0$, dim_{eff} maximal. Observable scaling: power-law (e.g., $\Gamma \sim n^{-3}$ for hydrogenic spectra, or analogous behaviour in nuclear level densities).
- **Prediction:** The exponent β_{eff} should change discontinuously at the HARD-to-Full transition.

This prediction is empirically testable using the existing UNNS corpus by comparing scaling exponents in near-boundary vs deep-interior ladders.

12.4 Observable Meaning of DOF Activation

Activation of additional effective degrees of freedom should appear observationally as one or more of:

- a new scaling exponent appearing in the observable response,
- a change in the asymptotic decay law (e.g., exponential \rightarrow power-law),
- a new symmetry channel becoming active,
- a modification of coupling structure (e.g., new independent coupling constant emerging),
- an increase in the number of independent correlation channels.

This turns DOF activation into something measurable, not merely formal.

13 Renormalization Interpretation of Structural Deformation

The deformation operator \hat{O}_α defines a renormalization-like flow on the admissibility manifold, driving structural states toward domain-specific fixed points while preserving spectral invariants.

The results of Section 9.3 and Section 11.1 together reveal a dynamical structure that admits a natural interpretation in terms analogous to renormalization group (RG) theory. We make this interpretation precise here, while clearly distinguishing the UNNS structural flow from conventional RG.

Definition 13.1 (Structural Flow Operator). The deformation operator \hat{O}_α induces a discrete flow on the three-coordinate structural state:

$$(\alpha_{\text{gs}}, m(L), \text{dim}_{\text{eff}}) \mapsto (\alpha'_{\text{gs}}, m(L)', \text{dim}'_{\text{eff}}),$$

with the fourth coordinate γ conserved. This flow is termed the *structural flow*. Its fixed points are the domain-specific attractors (m^*, dim^*) of Theorem 9.3.

Theorem 13.1 (Renormalization Flow Structure). *Under repeated application of \hat{O}_α , admissible ladders in the continuous convergence regime evolve toward fixed points:*

$$(\alpha_{\text{gs}}, m(L), \text{dim}_{\text{eff}}) \longrightarrow (\alpha_{\text{gs}}^*, m^*, \text{dim}^*),$$

with γ invariant throughout. The structural flow coordinates play the following roles:

- α_{gs} — *running parameter: driven toward α_{gs}^* exponentially (Theorem 9.9), analogous to a running coupling;*
- $m(L)$ — *stability coordinate: converges to m^* , measuring distance from the structural phase boundary;*
- dim_{eff} — *discrete phase observable: constant within a regime, jumps discretely at regime boundaries;*
- γ — *conserved quantity: invariant under the flow, analogous to a topological invariant preserved by RG.*

Proof sketch. The claim is a synthesis of Theorems 9.3, 9.9, and 9.6: the attractor provides the fixed point; exponential convergence provides the flow rate; and γ -invariance provides the conserved quantity. The discrete character of \dim_{eff} follows from the threshold structure of the DOF activation functional (Definition 4.1). \square \square

Theorem 13.2 (Fixed Points as Structural Universality Classes). *Each interaction regime (Section 8) corresponds to a structural universality class defined by the triple (γ, m^*, \dim^*) :*

- *Systems in the same γ -sector share the same spectral family and cannot be deformation-connected to systems in other sectors (Corollary 9.3);*
- *The attractor (m^*, \dim^*) is the fixed point of the structural flow within that sector;*
- *The interaction regime is the basin of attraction: all encodings of systems in the same regime converge to the same fixed point (Theorem 9.8).*

Theorem 13.3 (Discrete Phase Transitions as DOF Bifurcations). *Crossing a margin activation threshold induces a discrete jump:*

$$\dim_{\text{eff}} \longrightarrow \dim_{\text{eff}} + \Delta d, \quad \Delta d \in \mathbb{Z}_{>0}.$$

This is a structural phase transition — a bifurcation in the DOF activation functional — not a continuous deformation. Empirical instances: helium singlet ($\Delta d = 2$) and gold ($\Delta d = 1$) at $B = 0.01$ (corpus-supported, Section 11.1).

Remark 10 (UNNS Structural Flow vs Conventional RG). The structural flow of \hat{O}_α shares the fixed-point convergence and universality-class structure of conventional renormalization group flows, but differs in three important respects:

Conventional RG	UNNS Structural Flow
Acts on scale (energy/length)	Acts on gap structure
Purely continuous flow	Hybrid: continuous $(\alpha_{\text{gs}}, m(L))$ + discrete (\dim_{eff})
No guaranteed invariant exponent	γ invariant by Theorem 9.6
Geometry-based (metric / field)	Admissibility-based (gap covariance)
Fixed points at critical coupling	Fixed points at domain-specific (m^*, \dim^*)

The analogy is conceptually productive but must not be over-extended: the UNNS structural flow is defined on the admissibility manifold \mathcal{M}_{adm} , not on a field-theoretic configuration space, and the fixed points are attractor coordinates in (m, \dim) -space, not coupling constants at criticality.

14 Predictions and Falsifiability

The framework makes specific, falsifiable predictions:

1. **No direct detection of compactified dimensions.** Extra dimensions are not geometrically small but structurally suppressed. They cannot be “observed” by increasing energy alone; they require changing the structural regime (increasing $m(L)$).

2. **Regime transitions manifest as DOF activation.** Crossing a realizability boundary should produce a discrete increase in effective dimensionality, observable as new independent structural transformation axes becoming accessible.
3. **Sudden changes in coupling and scaling.** As new DOF activate, coupling constants and scaling exponents should change discontinuously — a structural phase transition.
4. **Symmetry activation under deformation.** Applying the α operator to near-boundary systems ($m(L) \approx 0$) should activate new symmetries as previously suppressed DOF become accessible.
5. **Dimensionality collapse at HARD boundary.** Systems approaching the HARD class ($m(L) = 0$) should exhibit reduced effective dimensionality, with only the minimal set of global DOF remaining.
6. **Exponent shift with DOF activation.** If two systems share similar $m(L)$ but differ in $\text{dim}_{\text{eff}}(L)$, they should exhibit different scaling exponents.
7. **Scaling transition with DOF change.** If a deformation increases $\text{dim}_{\text{eff}}(L)$, the system should show either: an exponent shift, a new correlation channel, or a change of asymptotic decay family.
8. **Compressed scaling near boundary.** Systems at or near $m(L) \rightarrow 0$ should show compressed scaling structure: fewer independent exponents, more global/degenerate response, boundary-dominated observables.
9. **New interaction regime requires distinct DOF profile.** A purported new interaction regime without a distinct DOF/scaling profile would falsify the framework.

Remark 11 (Falsification). The framework is falsified by any of:

- A physical system with $m(L) \gg 0$ that nevertheless exhibits lower effective dimensionality than a system with smaller $m(L)$.
- A system whose effective dimensionality changes without a corresponding change in $m(L)$ or realizability class.
- Observation of a new interaction regime that does not correspond to a distinct DOF activation profile.
- Two systems with identical $(\text{dim}_{\text{eff}}, m(L))$ that belong to different scaling families (contradicting the constraint that scaling family is determined by this pair).

15 Relation to Existing Theories

15.1 General Relativity

In the UNNS framework, spacetime geometry is not fundamental but emerges from structural admissibility. The metric tensor encodes the connectivity structure of the vulnerability graph. Dimensionality is not a property of spacetime but a signature of the accessible DOF set. This does not contradict GR — it provides a structural layer below it.

15.2 String Theory

String theory postulates extra dimensions to achieve mathematical consistency. The UNNS framework offers a different interpretation: what string theory calls “compactified dimensions” are degrees of freedom that are structurally suppressed because the system lies near a realizability boundary. The “scale” of compactification is the margin distance to that boundary. This reinterpretation does not invalidate string theory’s mathematical structure but relocates its physical interpretation.

15.3 Quantum Field Theory

The DOF activation functional provides a structural criterion for which field theoretic degrees of freedom are physically realisable. Not every field configuration is admissible; only those compatible with the margin constraints of the system.

16 Conclusion

We have established a structural derivation of dimensionality within the UNNS Substrate framework. The central argument is:

$$\underbrace{\text{UNNS admissibility}}_{\text{ordered gap sequence}} \longrightarrow \underbrace{m(L) > 0}_{\text{positive margin}} \longrightarrow \underbrace{\mathcal{D}(m(L), \bar{\rho}, \mathcal{R})}_{\text{DOF activation functional}} \longrightarrow \underbrace{\dim_{\text{eff}}(L) = |\mathcal{D}(m(L), \bar{\rho}, \mathcal{R})|}_{\text{effective dimensionality}}.$$

Within the UNNS framework, dimensionality is not a property of space but a derived observable of structural admissibility. The number of effective dimensions is determined by the set of admissible transformation axes selected by the connectivity margin. This reframes dimensionality from a geometric primitive to a regime-dependent structural invariant.

We have further extended the framework to observable scaling: effective dimensionality constrains the asymptotic scaling behaviour of admissible systems. The central claim is that scaling exponents, decay laws, and correlation families are selected not arbitrarily, but from a family determined by $(\dim_{\text{eff}}(L), m(L))$. Dimensionality thus becomes experimentally meaningful: not a geometric primitive, but a predictor of measurable scaling structure.

The framework:

- Explains why the observed dimensionality is not arbitrary — it is fixed by structural admissibility.
- Reinterprets extra dimensions as suppressed DOF, not geometrically small axes.
- Connects dimensionality directly to interaction regimes and operator response.
- Classifies operator action into three regimes (discrete activation, continuous convergence, inert) and establishes that each produces a distinct DOF evolution pattern (Theorems 9.2–9.5).
- Establishes the existence of domain-specific structural attractors and a universal margin band $m^* \in [0.553, 0.600]$ as a cross-domain fixed-point region of the deformation dynamics (Theorems 9.3–9.4).

- Identifies γ as a structural invariant coordinate that both preserves under deformation and stratifies the admissibility manifold into dynamically disconnected sectors (Theorems 9.6, 9.7; Corollary 9.3); completing a four-coordinate structural phase space $(\alpha_{\text{gs}}, m(L), \dim_{\text{eff}}, \gamma)$ with mixed dynamics (Corollary 9.2).
- Shows that encoding collapse is not neutral convergence but directed toward the maximum-margin canonical representation, elevating the Interaction Unification’s static selection criterion to a dynamical law (Principle 2; Corollary 9.4).
- Establishes that the universal margin attractor $m^* \in [0.553, 0.600]$ is regime-local — a fixed point within the strong-like interaction regime only — and scopes the universality claim accordingly (Theorem 9.10; Corollary 9.5).
- Makes falsifiable predictions about regime transitions, DOF activation, exponent shifts, and scaling changes under deformation.

What is solid. The derivation of $\dim_{\text{eff}}(L)$ from $m(L)$ and \mathcal{D} is definitional. The mapping to interaction regimes follows from the asymptotic classification of Φ . The consistency with corpus results (rigidity, commutativity, representation dependence, operator separation) is established. Monotonicity of DOF accessibility is Theorem 4.1. The threshold formulation (Equation 2) provides a clear computational model. The three-regime operator classification (Theorem 9.2) is supported by 35 systems across four domains. The universal margin band $m^* \in [0.553, 0.600]$ (Theorem 9.4), crystallographic attractor $\alpha_{\text{gs}}^* \approx 1.39$ (Theorem 9.3), and encoding collapse dynamics (Theorem 9.8) are corpus-supported. The γ stratification theorem (Theorem 9.7) upgrades invariance to manifold stratification; dynamic non-reachability across sectors follows as Corollary 9.3. Encoding collapse as maximum-margin directed selection is Principle 2. The regime-local scope of the margin band is established by Theorem 9.10 and Corollary 9.5.

What remains open. The explicit form of $m_{\text{min}}(\delta, \bar{\rho}, \mathcal{R})$ remains the primary unresolved formal object; the structural reasons for this are detailed in Section 11.2, which identifies three specific geometric gaps (directional metric, boundary hypersurface, differential response model) whose resolution would elevate the framework to a fully differential theory of dimensional emergence. The boundary of the “level-law-preserving” condition in Theorem 9.6 requires sharpening. Whether regime-local attractors exist in EM-like, weak-like, and gravity-like regime bands (Corollary 9.5) requires new corpus coverage. Threshold universality at $B=0.01$ across all three transitioning systems lacks formal explanation. Uniqueness of the structural attractor within each domain remains conjectural (Theorem 9.3).

What UNNS contributes. Traditional theories ask: how many dimensions does space have? UNNS reverses the question: given a physical system, what set of structural transformation axes does its margin allow? Dimensions are not properties of space — they are signatures of structural admissibility.

Within the UNNS framework, dimensionality is not a property of space but a derived observable of structural admissibility. The number of effective dimensions is determined by the set of admissible transformation axes selected by the connectivity margin.

A Proof of Theorem 5.1 (Detailed)

We provide the full proof of Theorem 5.1.

Part (i): Emergence. By Definition 3.1, a degree of freedom is defined as an admissible independent structural transformation axis in \mathcal{M}_{adm} . The admissibility manifold \mathcal{M}_{adm} is itself defined by the USL inequality. Therefore degrees of freedom are derived from the admissibility constraint, not assumed as primitives. Dimensionality, being the cardinality of this derived set, is similarly emergent.

Part (ii): Regime dependence. From Definition 4.1, $\mathcal{D}(m(L), \bar{\rho}, \mathcal{R})$ depends explicitly on $m(L)$ via the threshold condition $m(L) \geq m_{\text{min}}$. The Phase Mapping corpus establishes that $m(L)$ varies with the realizability class: Full systems have $m(L) \gg 0$; Tail systems have $m(L) \rightarrow 0$; HARD systems have $m(L) = 0$. Therefore $\dim_{\text{eff}}(L) = |\mathcal{D}(m(L), \bar{\rho}, \mathcal{R})|$ varies across regimes.

Part (iii): Structural determinacy. The margin $m(L)$ is computed directly from the gap sequence (Definition 2.3). The threshold $m_{\text{min}}(\delta, \bar{\rho}, \mathcal{R})$ depends on the ladder's position in \mathcal{M}_{adm} , which is determined by both $\bar{\rho}(L)$ and $\mathcal{R}(L)$. Therefore \mathcal{D} is computable from L , and $\dim_{\text{eff}}(L)$ is structurally determined. \square

B DOF Activation Functional: Threshold Form Derivation

The threshold formulation (Equation 2) is equivalent to the gradient-based form under the assumption that the directional sensitivity $\eta(\delta, \bar{\rho}, \mathcal{R})$ is inversely related to m_{min} :

$$m_{\text{min}}(\delta, \bar{\rho}, \mathcal{R}) = \frac{c}{\eta(\delta, \bar{\rho}, \mathcal{R})}$$

for some constant c . The threshold form is preferred for its computational interpretability: each structural direction δ has a characteristic minimum margin for activation.

For practical computation, we propose the following heuristic ansatz for m_{min} , included for computational illustration rather than as a derived expression:

$$m_{\text{min}}(\delta, \bar{\rho}, \mathcal{R}) = \frac{\sigma_{\delta}}{\Delta_{\text{ref}}} \cdot \exp\left(-\frac{d(\partial\Omega_L, \delta)}{L_0}\right),$$

where σ_{δ} is the directional gap variance, Δ_{ref} is a reference gap scale, $d(\partial\Omega_L, \delta)$ is the distance from the current state to the realizability boundary along direction δ , and L_0 is a correlation length. This ansatz captures the intuitive idea that directions with larger gap variance or greater distance to the boundary have higher activation thresholds. **This is a heuristic ansatz, not a derived expression, included for computational illustration.**

Instruments: STRUC-I v1.0.4 · STRUC-PERC-I v2.4.1 · Field Generator
v1.0 · `unns_scaling_extractor.py` · `transition_generator.py`

Pipeline: UNNS Dimensional Regime Synthesis Pipeline v1 (`atoms` · `condensed-matter` · `cosmo` ·
`crystallography`)